

Frequency domain electromagnetic data inversion

Caterina Fenu

Joint work with
Gian Piero Deidda and Giuseppe Rodriguez (University of Cagliari)

University of Pisa, Italy

PING Workshop, Florence,
April 6, 2016



Electromagnetic induction techniques

Electromagnetic induction (EMI) techniques are often used for non-destructive investigation of soil properties, as they are affected by electromagnetic properties of the subsurface layers, namely the electrical conductivity σ and the magnetic permeability μ .

Knowing such parameters allows one to ascertain the presence of particular substances, with many important applications:

- hydrological characterizations
- hazardous waste studies
- archaeological surveys
- precision-agriculture
- unexploded ordnance detection

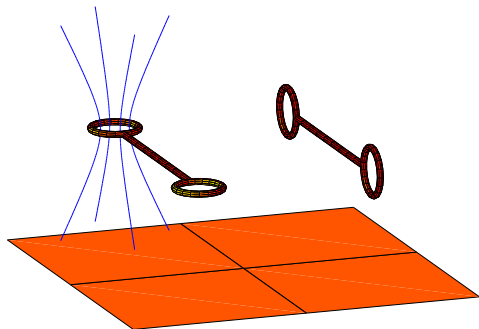
A **ground conductivity meter** is the basic instrument for EMI.

A (**GCM**) contains two coils (a transmitter and a receiver) placed at a fixed distance. An alternating sinusoidal current in the transmitter produces a primary magnetic field H_P , which induces small eddy currents in the subsurface. These currents produce a secondary magnetic field H_S , which is sensed by the receiver.

The ratio of the secondary to the primary magnetic fields is then used, along with the instrumental parameters, to estimate electrical properties of the subsurface.

Ground conductivity meter

The coils axes can be aligned either vertically or horizontally with respect to the ground surface, producing different measures.



vertical & horizontal alignments

Ground conductivity meter

Under some assumptions:

- instrument at ground level ($h = 0$), in vertical orientation,
- soil with uniform magnetic permeability $\mu_0 = 4\pi 10^{-7}$ H/m,
- soil with uniform electrical conductivity σ ,
- small induction number

$$B = r \sqrt{\frac{1}{2} \mu_0 \omega \sigma} \ll 1,$$

where

- r is the inter-coil distance (~ 1 m),
- $\omega = 2\pi f$, f operating frequency (~ 10 kHz).

Ground conductivity meter

Under some assumptions:

- instrument at ground level ($h = 0$), in vertical orientation,
- soil with uniform magnetic permeability $\mu_0 = 4\pi 10^{-7}$ H/m,
- soil with uniform electrical conductivity σ ,
- small induction number

$$B = r \sqrt{\frac{1}{2} \mu_0 \omega \sigma} \ll 1,$$

the instruments measures the apparent conductivity

$$m = \frac{4 \operatorname{Im}(H_S/H_P)}{\mu_0 \omega r^2},$$

which, under the above assumptions, coincides with σ .

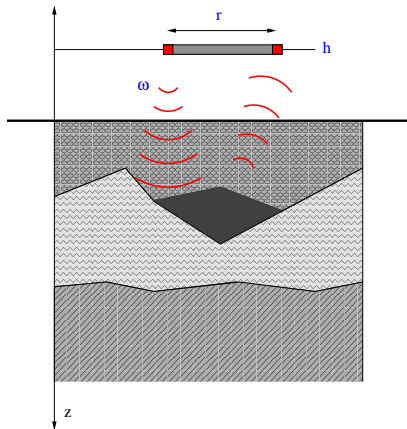
The inversion problem

In real applications the assumption of uniform soil conductivity is not realistic. On the contrary, geophysicists are particularly interested in non homogeneous soil.

Moreover, apparent conductivity gives no information on the depth localization of inhomogeneities.

To face the problem of data inversion multiple measures are needed to recover the distribution of conductivity with respect to depth.

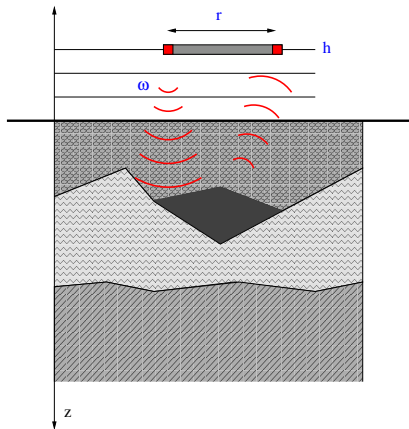
Parameters which influence the GCM measures



- orientation (vert/horiz)
- height over the ground h
- inter-coil distance r
- angular frequency ω

they can be varied in order to generate multiple measures for each geographical position, and realize data inversion

Parameters which influence the GCM measures



- orientation (vert/horiz)
- height over the ground h
- inter-coil distance r
- angular frequency ω

measurements are taken for

$$h = h_k = (k - 1)\Delta h$$

for $k = 1, \dots, 20$, $\Delta h = 0.1$ m

The linear model

In 1980, McNeill (Geonics) described a linear model, based on the *response curves* in the vertical and horizontal positions, which relates the apparent conductivity to the height over the ground

$$m^V(h) = \int_0^{\infty} \phi^V(h+z)\sigma(z) dz$$
$$m^H(h) = \int_0^{\infty} \phi^H(h+z)\sigma(z) dz$$

where $\sigma(z)$ is the real conductivity,

$$\phi^V(z) = \frac{4z}{(4z^2 + 1)^{3/2}}, \quad \phi^H(z) = 2 - \frac{4z}{(4z^2 + 1)^{1/2}},$$

and z is the ratio between the depth and the inter-coil distance r .

The linear model

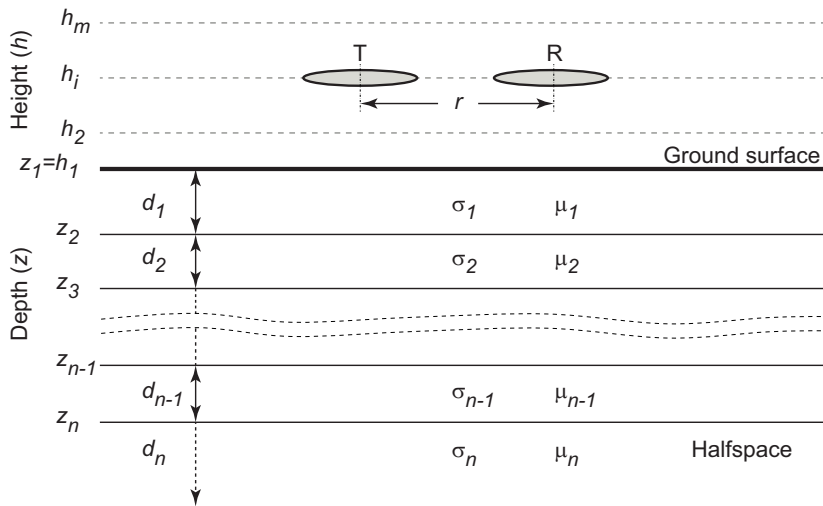
In 1980, McNeill (Geonics) described a linear model, based on the *response curves* in the vertical and horizontal positions, which relates the apparent conductivity to the height over the ground

$$m^V(h) = \int_0^{\infty} \phi^V(h+z)\sigma(z) dz$$
$$m^H(h) = \int_0^{\infty} \phi^H(h+z)\sigma(z) dz$$

The linear model is valid for:

- uniform magnetic permeability $\mu_0 = 4\pi 10^{-7}$ H/m,
- small *induction number*,
- **moderate conductivity** ($\sigma \lesssim 100$ mS/m).

The nonlinear model [Wait 1982], [Hendrickx et al 2002]



The nonlinear model

The **electric conductivity** $\sigma(z)$ and **magnetic permeability** $\mu(z)$ are assumed to be piecewise constant (i.e., layered soil)

$$\sigma = \sigma_0, \sigma_1, \dots, \sigma_m, \quad \mu = \mu_0, \mu_1, \dots, \mu_m,$$

in each layer of width d_k (σ_0, μ_0 in free space).

The model is derived from **Maxwell's equations**, keeping into account the **cylindrical symmetry** of the problem, (H at the receiver is independent of the vertical rotation of the GCM).

Let the **characteristic admittance** inside the k th layer be

$$N_k(\lambda) = \frac{u_k(\lambda)}{i\mu_k\omega}, \quad u_k(\lambda) = \sqrt{\lambda^2 + i\sigma_k\mu_k\omega},$$

for $k = 0, 1, \dots, m$, where λ has no direct physical meaning.

The nonlinear model

The **surface admittance** Y_k at the top of the k -th layer can be obtained by the following recursion

$$Y_k(\lambda) = N_k(\lambda) \frac{Y_{k+1}(\lambda) + N_k(\lambda) \tanh(d_k u_k(\lambda))}{N_k(\lambda) + Y_{k+1}(\lambda) \tanh(d_k u_k(\lambda))},$$

setting $Y_m(\lambda) = N_m(\lambda)$ at the lowest layer
and letting $k = m - 1, m - 2, \dots, 1$.

Let the **reflection factor** be

$$R_0(\lambda) = \frac{N_0(\lambda) - Y_1(\lambda)}{N_0(\lambda) + Y_1(\lambda)}.$$

Then, the (vert/horiz) **apparent conductivity** is given by

$$m^V(\sigma, \mu; h) = \frac{4r}{\mu_0\omega} \mathcal{H}_0 \left[-\lambda e^{-2h\lambda} \operatorname{Im}(R_0(\lambda)) \right] (r)$$

$$m^H(\sigma, \mu; h) = \frac{4}{\mu_0\omega} \mathcal{H}_1 \left[-e^{-2h\lambda} \operatorname{Im}(R_0(\lambda)) \right] (r)$$

where h is the height above the ground. We denote by

$$\mathcal{H}_\nu[f](r) = \int_0^\infty f(\lambda) J_\nu(r\lambda) \lambda d\lambda, \quad \nu = 1, 2,$$

the Hankel transform, while J_0, J_1 are first kind Bessel functions.

Inversion of the nonlinear model

We consider the residual vector

$$\mathbf{r}(\boldsymbol{\sigma}) = \mathbf{b} - \mathbf{m}(\boldsymbol{\sigma}),$$

as a function of the conductivities $\boldsymbol{\sigma} = (\sigma_1, \dots, \sigma_n)^T$, where

$$r_i(\boldsymbol{\sigma}) = \begin{cases} b_i^V - m^V(\boldsymbol{\sigma}, h_i), & i = 1, \dots, m, \\ b_{i-m}^H - m^H(\boldsymbol{\sigma}, h_{i-m}), & i = m + 1, \dots, 2m, \end{cases}$$

b_i^V, b_i^H ($i = 1, \dots, m$) are the V/H measurements and $m^{V/H}(\boldsymbol{\sigma}, h)$ are the V/H apparent conductivities at height h .

In our analysis, we let the magnetic permeability take the same value μ_0 in the n layers. This assumption is approximately met if the ground does not contain ferromagnetic materials.

Inversion by Newton's method

The problem of data inversion consists of computing the conductivity σ_i of each layer which determine a given data set $\mathbf{b} \in \mathbb{R}^{2m}$, i.e.,

$$\min_{\boldsymbol{\sigma} \in \mathbb{R}^n} f(\boldsymbol{\sigma}), \quad \text{with } f(\boldsymbol{\sigma}) = \frac{1}{2} \|\mathbf{r}(\boldsymbol{\sigma})\|^2,$$

Newton's method consists of the iteration $\boldsymbol{\sigma}_{k+1} = \boldsymbol{\sigma}_k + \mathbf{s}_k$, where \mathbf{s}_k solves the linear system

$$\mathbf{f}''(\boldsymbol{\sigma}_k)\mathbf{s} = -\mathbf{f}'(\boldsymbol{\sigma}_k).$$

While $\mathbf{f}'(\boldsymbol{\sigma})$ is available, **computing $\mathbf{f}''(\boldsymbol{\sigma})$ is hard.**

The **Gauss–Newton** method is based on the least squares minimization of a linear approximation of $\mathbf{r}(\boldsymbol{\sigma}_{k+1}) = \mathbf{r}(\boldsymbol{\sigma}_k + \mathbf{s})$

$$\min_{\mathbf{s} \in \mathbb{R}^n} \|\mathbf{r}(\boldsymbol{\sigma}_k) + J_k \mathbf{s}\|,$$

where $J_k = J(\boldsymbol{\sigma}_k) = \left(\frac{\partial r_i(\boldsymbol{\sigma}_k)}{\partial \sigma_j} \right)$, or some approximation.

Armijo–Goldstein principle

The iteration becomes

$$\boldsymbol{\sigma}_{k+1} = \boldsymbol{\sigma}_k + \alpha_k \mathbf{s}_k = \boldsymbol{\sigma}_k - \alpha_k J_k^\dagger \mathbf{r}(\boldsymbol{\sigma}_k),$$

where J_k^\dagger is the Moore–Penrose pseudoinverse of J_k and α_k is a **damping parameter** determined by **Armijo–Goldstein** principle, that is, α_k as the largest number in the sequence 2^{-i} , $i = 0, 1, \dots$, for which the following inequality holds

$$\|\mathbf{r}(\boldsymbol{\sigma}_k)\|^2 - \|\mathbf{r}(\boldsymbol{\sigma}_k + \alpha_k \mathbf{s}_k)\|^2 \geq \frac{1}{2} \alpha_k \|J_k \mathbf{s}_k\|^2.$$

This choice of α_k ensures convergence of the method, provided that $\boldsymbol{\sigma}_k$ is not a critical point and allows us to obtain positive solutions.

Newton

$$\mathbf{f}''(\boldsymbol{\sigma}_k)\mathbf{s} = -\mathbf{f}'(\boldsymbol{\sigma}_k)$$

Gauss–Newton

$$J_k^T J_k \mathbf{s} = -J_k^T \mathbf{r}(\boldsymbol{\sigma}_k)$$

We have

$$\mathbf{f}'(\boldsymbol{\sigma}) = J(\boldsymbol{\sigma})^T \mathbf{r}(\boldsymbol{\sigma})$$

$$\mathbf{f}''(\boldsymbol{\sigma}) = J(\boldsymbol{\sigma})^T J(\boldsymbol{\sigma}) + \sum_{i=1}^{2m} r_i(\boldsymbol{\sigma}) H_i(\boldsymbol{\sigma})$$

where $[H_i(\boldsymbol{\sigma})]$ is the Hessian of the i th residual $r_i(\boldsymbol{\sigma})$.

The **additional term** is neglectable if each $r_i(\boldsymbol{\sigma})$ is either **small** (compatible problem) or **mildly nonlinear** at $\boldsymbol{\sigma}_k$.

Computation of the Jacobian matrix - 1

To obtain derivatives $Y'_{kj} = \frac{\partial Y_k}{\partial \sigma_j}$ ($k, j = 1, \dots, n$) we start from

$$Y'_{nn} = \frac{1}{2u_n}, \quad Y'_{nj} = 0, \quad j = 1, \dots, n-1,$$

and proceeding recursively for $k = n-1, n-2, \dots, 1$ by

$$\begin{aligned} Y'_{kj} &= N_k^2 b_k Y'_{k+1,j}, \quad j = n, n-1, \dots, k+1, \\ Y'_{kk} &= \frac{a_k}{2u_k} + \frac{b_k}{2} \left[N_k^2 d_k - Y_{k+1} \left(d_k Y_{k+1} + \frac{1}{i\mu_k \omega} \right) \right], \\ Y'_{kj} &= 0, \quad j = k-1, k-2, \dots, 1. \end{aligned}$$

All functions of λ are complex valued, and

$$a_k = \frac{Y_{k+1} + N_k \tanh(d_k u_k)}{N_k + Y_{k+1} \tanh(d_k u_k)}, \quad b_k = \frac{1}{[N_k + Y_{k+1} \tanh(d_k u_k)]^2 \cosh^2(d_k u_k)}.$$

Computation of the Jacobian matrix - 1

To obtain derivatives $Y'_{kj} = \frac{\partial Y_k}{\partial \sigma_j}$ ($k, j = 1, \dots, n$) we start from

$$Y'_{nn} = \frac{1}{2u_n}, \quad Y'_{nj} = 0, \quad j = 1, \dots, n-1,$$

and proceeding recursively for $k = n-1, n-2, \dots, 1$ by

$$\begin{aligned} Y'_{kj} &= N_k^2 b_k Y'_{k+1,j}, \quad j = n, n-1, \dots, k+1, \\ Y'_{kk} &= \frac{a_k}{2u_k} + \frac{b_k}{2} \left[N_k^2 d_k - Y_{k+1} \left(d_k Y_{k+1} + \frac{1}{i\mu_k \omega} \right) \right], \\ Y'_{kj} &= 0, \quad j = k-1, k-2, \dots, 1. \end{aligned}$$

Numerical implementation needs care:

- **cancellation** may occur in some formulae arrangement;
- **NaNs** appear for large λ 's, because of $\cosh(\sqrt{z})$ with $z \in \mathbb{C}$.

Finally,

$$\frac{\partial m^V(h)}{\partial \sigma_j} = \frac{4r}{\mu_0 \omega} \mathcal{H}_0 \left[\lambda e^{-2h\lambda} \operatorname{Im} \left(\frac{\partial R_0(\lambda)}{\partial \sigma_j} \right) \right] (r),$$
$$\frac{\partial m^H(h)}{\partial \sigma_j} = \frac{4}{\mu_0 \omega} \mathcal{H}_1 \left[e^{-2h\lambda} \operatorname{Im} \left(\frac{\partial R_0(\lambda)}{\partial \sigma_j} \right) \right] (r),$$

where

$$\frac{\partial R_0(\lambda)}{\partial \sigma_j} = \frac{\partial}{\partial \sigma_j} \frac{N_0(\lambda) - Y_1(\lambda)}{N_0(\lambda) + Y_1(\lambda)} = \frac{-2i\mu_0\omega\lambda}{(\lambda + i\mu_0\omega Y_1(\lambda))^2} \cdot \frac{\partial Y_1}{\partial \sigma_j}.$$

The complexity is lower than using the finite differences approach.

Finite difference approximation

$$\frac{\partial r_i}{\partial \sigma_j}(\boldsymbol{\sigma}) = \frac{r_i(\boldsymbol{\sigma} + \boldsymbol{\delta}_j) - r_i(\boldsymbol{\sigma})}{\delta},$$

where $\boldsymbol{\delta}_j = \delta \mathbf{e}_j = (0, \dots, 0, \delta, 0, \dots, 0)^T$,

for $i = 1, \dots, 2m$ and $j = 1, \dots, n$;

$2m$ is the size of the data set and n the number of layers.

This is the approach used in the existing package for nonlinear inversion (`em38nonlin`).

Computing the Jacobian is about 5 times faster.

Broyden update

Starting with $J_0 = J(\boldsymbol{\sigma}_0)$, we set

$$J_k = J_{k-1} + \frac{(\mathbf{y}_k - J_{k-1}\mathbf{s}_k)\mathbf{s}_k^T}{\mathbf{s}_k^T \mathbf{s}_k},$$

where $\mathbf{s}_k = \boldsymbol{\sigma}_k - \boldsymbol{\sigma}_{k-1}$ and $\mathbf{y}_k = r(\boldsymbol{\sigma}_k) - r(\boldsymbol{\sigma}_{k-1})$.

This formula makes the linearization

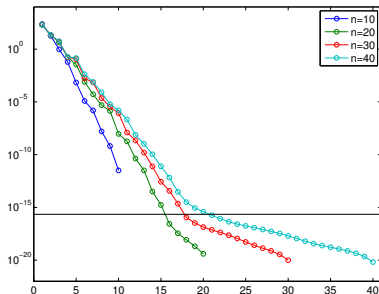
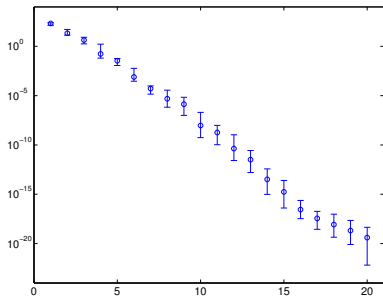
$$r(\boldsymbol{\sigma}_k) + J_k(\boldsymbol{\sigma} - \boldsymbol{\sigma}_k)$$

exact in $\boldsymbol{\sigma}_{k-1}$, and guarantees the least change in $\|J_k - J_{k-1}\|_F$.

The update makes the computation 5 times faster.

The problem is ill-conditioned, regularization is needed.

Let $J(\sigma_k) = U\Sigma V^T$, $\sigma_k = 100 \cdot \text{rand}(n, 1)$, $k = 1, \dots, 1000$.



- Left-side: average singular values and errors ($n = 20$).
- Right-side: average singular values for $n = 10, 20, 30, 40$.

The conditioning increases with dimension and does not change much during iteration.

Nonlinear regularization method: TSVD approach

We replace the ill-conditioned Jacobian $J = J_k$ with the **best rank ℓ approximation** according to the Euclidean norm

$$A_\ell = \min_{\text{rank}(A)=\ell} \|J - A\|_2.$$

Let $J = U\Gamma V^T$ and $p = \text{rank}(J)$. Then, the **regularized Gauss-Newton step** vector $\mathbf{s}^{(\ell)}$ can be expressed as

$$\mathbf{s}^{(\ell)} = -A_\ell^\dagger \mathbf{r}(\sigma_k) = -\sum_{i=1}^{\ell} \frac{\mathbf{u}_i^T \mathbf{r}(\sigma_k)}{\gamma_i} \mathbf{v}_i,$$

where $\ell = 1, \dots, p$ is the regularization parameter.

Using a regularization matrix: TGSVD

Let us introduce a regularization matrix $L \in \mathbb{R}^{t \times n}$ ($t \leq n$).
Common choices are $L = D_1, D_2$.

We call *minimal L-norm solution* the vector which solves

$$\min_{\mathbf{s} \in \mathcal{S}} \|\mathbf{L}\mathbf{s}\|, \quad \mathcal{S} = \{\mathbf{s} \in \mathbb{R}^n \mid \mathbf{J}^T \mathbf{J} \mathbf{s} = -\mathbf{J}^T \mathbf{r}(\sigma_k)\},$$

under the assumption $\mathcal{N}(\mathbf{J}) \cap \mathcal{N}(\mathbf{L}) = \{0\}$.

By the *generalized singular value decomposition* (GSVD) of (\mathbf{J}, \mathbf{L})

$$\mathbf{J} = \mathbf{U} \Sigma_{\mathbf{J}} \mathbf{Z}^{-1}, \quad \mathbf{L} = \mathbf{V} \Sigma_{\mathbf{L}} \mathbf{Z}^{-1},$$

it is possible to define the **truncated GSVD (TGSVD) solution** \mathbf{s}_ℓ ,
where $\ell = 0, 1, \dots, \bar{p}$ is the **regularization parameter**
and \bar{p} depends upon p and t .

Inversion algorithm

We apply the regularized damped Gauss–Newton method

$$\boldsymbol{\sigma}_{k+1}^{(\ell)} = \boldsymbol{\sigma}_k^{(\ell)} + \alpha_k \mathbf{s}_k^{(\ell)} = \boldsymbol{\sigma}_k^{(\ell)} - \alpha_k \mathbf{A}_\ell^\dagger \mathbf{r}(\boldsymbol{\sigma}_k^{(\ell)}),$$

with ℓ fixed, α_k determined by Armijo–Goldstein/positivity.

We iterate until

$$\|\boldsymbol{\sigma}_k^{(\ell)} - \boldsymbol{\sigma}_{k-1}^{(\ell)}\| < \tau \|\boldsymbol{\sigma}_k^{(\ell)}\| \quad \text{or} \quad k > 100 \quad \text{or} \quad \alpha_k < 10^{-5},$$

for a given τ . The solution at convergence is denoted by $\boldsymbol{\sigma}^{(\ell)}$.

The choice of the regularization parameter ℓ is crucial.

Not all the methods for determining a regularization parameter available for linear problems can be adapted to the nonlinear case.

The optimal choice would be the **discrepancy principle**

$$\|\mathbf{b} - \mathbf{m}(\sigma^{\ell_{\text{discrepancy}}})\| \leq \kappa \|\mathbf{e}\|, \quad \kappa > 1,$$

but it can seldom be applied to EMI techniques because in applications

- the noise on the data is not necessarily equally distributed,
- an accurate estimate of $\|\mathbf{e}\|$ is often unknown.

Choosing ℓ : L-curve

Among the *heuristic* methods, which do not require an estimate of $\|\mathbf{e}\|$, the **L-curve principle** [Hansen, O'Leary 1993] can be adapted quite naturally to the nonlinear case.

It chooses the value of ℓ which identifies the *corner* of the curve connecting the points

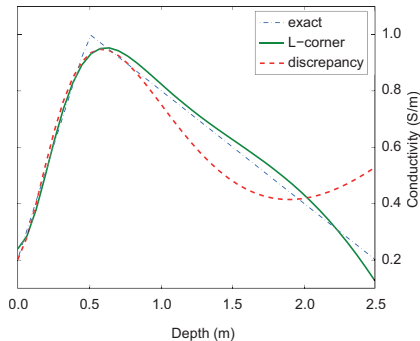
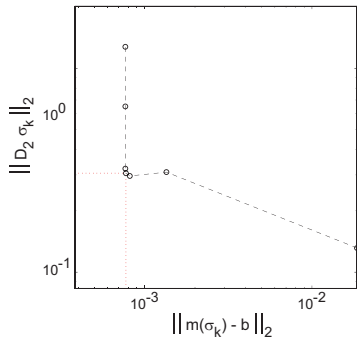
$$\left\{ \log \|\mathbf{r}(\boldsymbol{\sigma}^{(\ell)})\|, \log \|L\boldsymbol{\sigma}^{(\ell)}\| \right\}, \quad \ell = 1, \dots, \bar{p}.$$

The curve is L-shaped in many discrete ill-posed problems.

To detect the corner of the L-curve we used two algorithms:

- the **L-corner** method [Hansen, Jensen, Rodriguez 2007];
- the **ResReg** method [Regińska 1996], [Reichel, Rodriguez 2013].

Experimental results with synthetic data

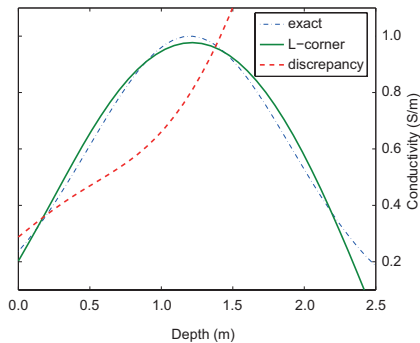
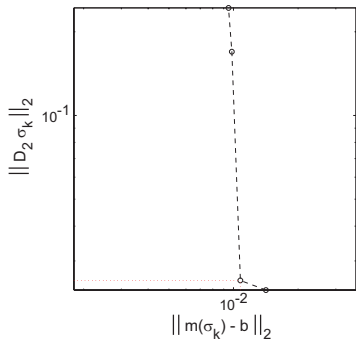


piecewise linear conductivity distribution

10+10 measurements, 40 layers, noise 10^{-3} , $L = D_1$

$l_{\text{optimal}} = 4$, $l_{\text{L-corner}} = 3$, $l_{\text{discrepancy}} = 2$

Experimental results with synthetic data

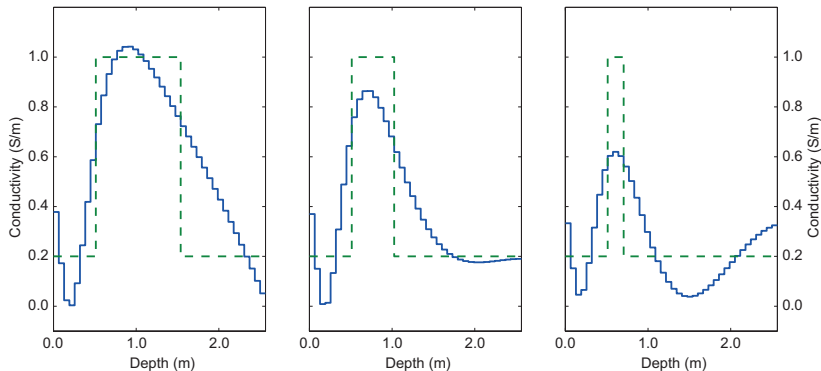


smooth conductivity distribution

10+10 measurements, 40 layers, noise 10^{-2} , $L = D_2$

$\ell_{\text{optimal}} = 2$, $\ell_{\text{L-corner}} = 2$, $\ell_{\text{discrepancy}} = 1$

Experimental results with synthetic data



identification of thin conductive layers

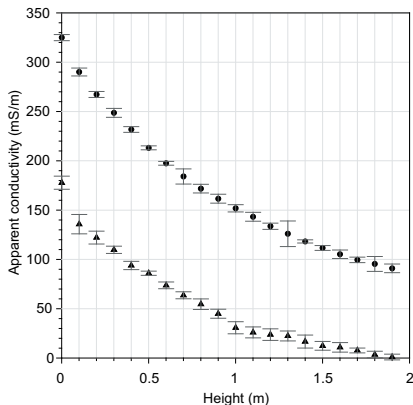
$$f_{\xi}(z) = 1 \text{ for } z \in [0.5, 0.5 + \xi] \quad \xi = 1.0, 0.5, 0.2$$

10+10 measurements, 40 layers, noise 10^{-2} , $L = D_1$

Experiments on field data: the Airport data set

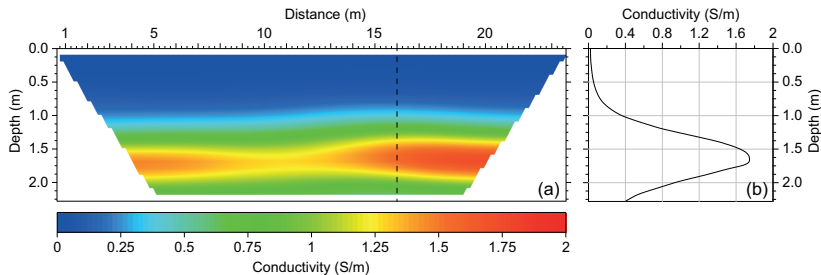


Experiments on field data: the Airport data set



20 measurements for each $h_i = 0, 0.1, \dots, 1.9$ m
error bars are standard deviations (multiplied by 10)

Experiments on field data: the Airport data set



Electrical resistivity tomography (ERT)

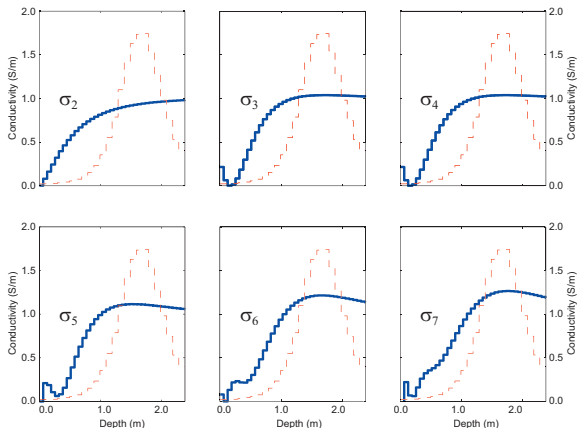
Iris Instruments Syscal Pro Switch 48 resistivity meter
48 electrodes set up with an inter-electrode spacing of 0.5 m

There is a conductivity maximum at depth ~ 1.6 m

EM data measured at $x = 16$ m

GF Instruments CMD-1 conductivity meter
operating frequency 10 kHz, coil separation 0.98 m

Experiments on field data: the Airport data set

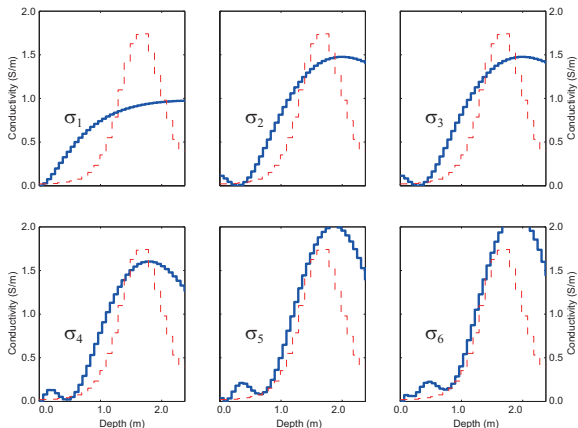


Gauss-Newton solutions - ERT conductivity profile

20+20 measurements, 40 layers, $L = I$

$l_{L\text{-corner}} = 5$, $l_{\text{ResReg}} = 4$

Experiments on field data: the Airport data set

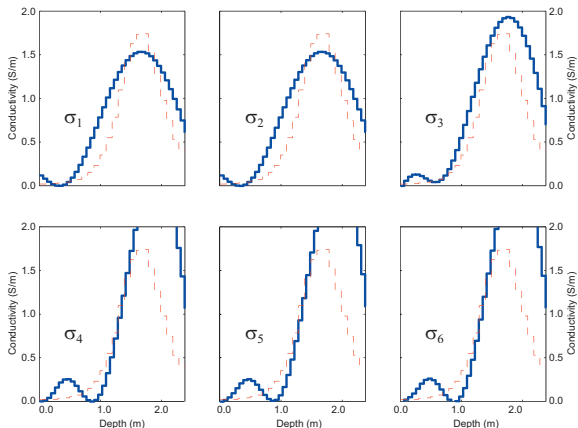


Gauss-Newton solutions - ERT conductivity profile

20+20 measurements, 40 layers, $L = D_1$

$l_{L\text{-corner}} = 2$, $l_{\text{ResReg}} = 1$

Experiments on field data: the Airport data set

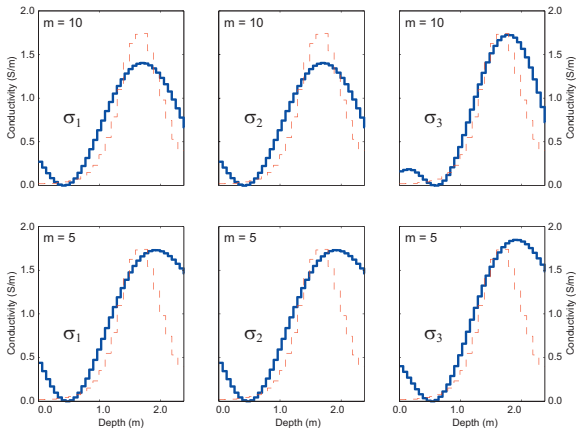


Gauss-Newton solutions - ERT conductivity profile

20+20 measurements, 40 layers, $L = D_2$

$l_{L\text{-corner}} = 2$, $l_{\text{ResReg}} = 1$

Experiments on field data: the Airport data set



Gauss-Newton solutions - ERT conductivity profile
10+10 and 5+5 measurements, 40 layers, $L = D_2$, $\ell_{L\text{-corner}} = 2$

Numerical experiments showed that:

- a small number of solutions σ^ℓ has to be computed
- the *L-corner* method produces acceptable solutions
- meaningful results can be obtained with $m = 5$
- Broyden update is extremely effective
- computation is very fast even on a notebook
- $L = D_1, D_2$ better than $L = I$

In the future:

- work with multifrequency/multi intercoil distance GCM measurements
- consider also the variation of the magnetic permeability
- consider also the “in-phase component” of the signal

